DESCRIPTION OF MECHANICAL RESPONSE INCLUDING DETACHMENT USING A NOVEL PARTICLE MODEL OF BIOFILM/FLOW INTERACTION

Erik Alpkvist1*, Isaac Klapper2,

1 Applied Mathematics Group, School of Technology and Society, Malmö University, SE-20506 Malmö, Sweden.

2 Department of Mathematical Sciences & Center for Biofilm Engineering
Montana State University, Bozeman, Montana 59717

ABSTRACT

Bacterial biofilms, while made up of microbial-scale objects, also function as meso- and macro-scale materials. In particular, macro-scale material properties determine how biofilms respond to large-scale mechanical stresses, e.g., fluid shear. Viscoelastic and other constitutive properties influence biomass structure (through growth and fluid shear stresses) by erosion and sloughing detachment. In this paper, using the immersed boundary method, biofilm is modeled by a system of viscoelastic, breakable springs embedded in a fluid flow, evolving according to the basic physical laws of conservation of mass and momentum. We demonstrate *in silico* biofilm deformation and detachment under fluid shear stress.

KEYWORDS

Biofilm model, immersed boundary method, detachment, sloughing, streamers.

INTRODUCTION

Over long time scales, biofilms exist in a stationary state where material gains from growth are balanced on average by material losses through a number of possible mechanisms. Among the most important of those mechanisms are mechanically induced ones, e.g. fluid mediated transport and detachment via erosion and sloughing. Much effort in biofilm modeling (e.g. Alpkvist *et al.* (2006) Alpkvist and Klapper 2006, Kreft *et al.* (1998), Dockery and Klapper (2002), Picioreanu (1998)) has focused on growth. Less attention however has been directed to the mechanics of detachment. In this paper, we propose use of the immersed boundary (IB) method as a framework for studying bulk fluid-driven mechanical stress in biofilms and subsequent induced detachment.

Biofilm as a material can be characterized as a viscoelastic fluid, Klapper *et al.* (2001), with quantitatively measurable material properties, see Shaw *et al.* (2004), Wloka *et al.* (2004), and Stoodley *et al.* (2002). In particular, on short time scales (compared to the elastic relaxation time, see Shaw et al. (2004)) biofilm acts as an elastic solid, while on longer time scales biofilm acts as a viscous fluid. The combination of behaviors, complex by themselves, makes study of biofilm mechanics especially difficult. Thus, although flow-biomass interaction or detachment has been occasionally considered (Dillon *et al.* (1996), Picioreanu *et al.* (2001), Cogan *et al.* (2006) and

Chambless *et al.* (2006)) it is usually not included in models, and in fact observed viscoelastic properties have not yet been described by a model that can provide a complete material description. While as a general rule biofilm models are easier to construct than biofilm experiments, in this instance the opposite may be true - description and implementation of biofilm constitutive properties is a difficult task. Nevertheless, experimental observations suggest important physical questions that seem to require modeling studies to answer satisfactorily: are streamers formed by material stretching, and if so, how? And what might be their effect on fluid drag? Why do biofilms form ripples and, more generally, how important is material transport (of biofilm) in structure? And, most importantly, how does shear stress distribute through the biofilm and how does this distribution affect biofilm detachment? Here, we focus on presentation and constructing of a modeling frame-work capable of addressing these issues.

The IB method, a popular computational technique for coupling of fluid flow to elastic materials dates back almost 30 years to the work by Peskin (1977). Originally it was developed as a tool to describe blood flow-muscle interactions in the dynamic heart. The method will be outlined here but for a more complete description based upon calculus of variations see Peskin (2002). Over the years IB has been extensively applied to various biological problems, for example, the viscoelastic network model by Bottino (1998), the model of platelet thrombosis by Fogelson and Guy (2004), or the micro-scale biofilm model by Dillon *et al.* (1996). IB allows problems with complicated boundaries and interfaces to be embedded in rectangular or periodic domains, a favorable geometry for computations. Here, we adapt the immersed boundary method to study biomass-fluid flow interaction of a mature biofilm.

METHODS

Modeling

Consider a biofilm in a three dimensional (3D) channel Ω described by coordinates **x**=(x,y,z). Channel "floor"' and "ceiling" are located at z=0 and z=300μm respectively. For simplicity we assume periodic boundary conditions in the x and y directions. The bottom plate at z=0 is held steady. In order to drive fluid flow through the system, the top plate is moved with an imposed velocity [U(t),0,0] in the x-direction. In two dimensional (2D) examples we suppress variation in the y-direction, i.e., transverse to the principle direction of flow. Motion in the biomass-bulk fluid system is characterized by the velocity field **u**=[u(t,x), v(t,x), w(t,x)] which in turn is governed by the Navier-Stokes equations (Landau (1967))

$$\frac{\partial \mathbf{u}}{\partial t} + (\mathbf{u}\cdot\nabla)u = -\frac{1}{\rho}\nabla p + \nu\nabla^2\mathbf{u} + \frac{1}{\rho}\mathbf{F},\ x \in \Omega \qquad (1)$$

$$\nabla\cdot\mathbf{u} = 0, x \in \Omega \qquad (2)$$

where (1) is the balance of inertial, pressure, viscous, and viscoelastic forces, and (2) is incompressibility-induced mass balance. p=p(t,**x**) is the pressure, **u**=**u**(t,**x**) the flow field, **F**=**F**(t,**x**) the internal viscoelastic force density within the fluid-biofilm system - in 2D force per unit area and in 3D force per volume. ρ and ν are the density and the kinematic viscosity of water. Macroscopic behavior of the biofilm depends on microscopic forces and is coupled to the flow of biomass and liquid through the function **F** in (1). Following the principles of the IB method, microscopic forces are coupled to the fluid motion in such a way as to enforce mass and force balances for the entire system.

The immersed boundary method

The immersed boundary method provides a way to embed an elastic (or viscoelastic) membrane or body within a viscous fluid. The advantage of such an approach is that one can solve for behavior of

the entire mixed-material domain by solving the Navier-Stokes equations only, an especially useful property if the overall domain can be made rectangular. In such geometries there are many simple and efficient Navier-Stokes solvers available.

Following IB, we discretize the biofilm region into a number of nodes. Within our numerical framework, we have developed a robust method of testing various biofilm shapes. The discretization procedure is illustrated in Figure 1. Nodes are distributed in a hexagonal pattern covering the area in 2D or volume in 3D, occupied by biofilm. Then each node is displaced by a rectangle distributed perturbation with standard deviation of $0.8d_0$, were d_0 is characteristic length scale of the springs at rest defined later on, as in Bottino (1998).

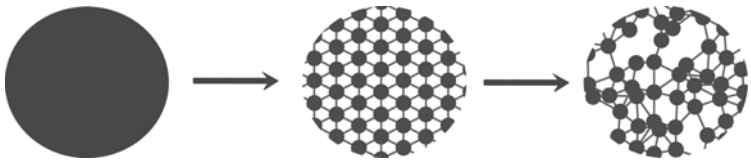

Figure 1. A circular biofilm region is discretized into an ordered network of springs and particles and then perturbed.

Suppose now the biofilm region is discretized into N_p particles and set $\mathbf{X}_n=\mathbf{X}_n(t)$ to be the position in space as a function of time of the n'th particle such that $\mathbf{X}=(X_n(t),Y_n(t),Z_n(t))$ are the coordinates for the particle in a lagrangian coordinate system.. We introduce a network of generalized springs connecting biomass particles, see Figure 1, with resulting net force on the n'th particle given by $\mathbf{f}_n=\mathbf{f}_n(t)$. Details of the spring forcing will be given below. A key idea of the immersed boundary method is that a force at a point (x_i,y_j,z_k) in an eulerian grid of N_i, N_j and N_k gridpoints along x, y and z respectively may be written as

$$\mathbf{F}(x_i,y_j,z_k)=\int\int\int \mathbf{F}(x,y,z)\partial(x_i-x)\partial(y_j-y)\partial(z_k-z)dxdydz \tag{3}$$

where $\delta=\delta(\mathbf{x})$ is a dirac distribution function. Thus, using a discretized version of equation (3), we may describe the approximate force at a point on the fluid grid arising from the forces at the moving nodes:

$$\mathbf{F}_{i,j,k}=\sum_{n=1}^{N_p}\mathbf{f}_n(t)\delta_h((x_i-X_n)/h)\delta_h((y_j-Y_n)/h)\delta_h((z_k-Z_n)/h)\mathrm{d}_0^3 \tag{4}$$

where δ_h and h is a numerical Dirac delta function and the eulerian gridsize. A smoothed numerical Dirac delta function can be chosen as (Peskin (2002))

$$\delta_h(r)\begin{cases}(3-2|r|-\sqrt{1+4|r|-4r^2})/8/h, & |r|\le 1\\ (5-2|r|-\sqrt{-7+12|r|-4r^2})/8/h, & |r-3/2|\le 1\\ 0, & |r|>2.\end{cases} \tag{5}$$

The velocities of the particles can be interpolated from eulerian grid by:

$$\frac{d\mathbf{X}_n}{dt}=\sum_{i,j,k=0}^{N_i,N_j,N_k}u(x_i,y_j,z_k,t)\delta_h((X_n-x_i)/h)\delta_h((X_n-x_i)/h)\delta_h((X_n-x_i)/h)h^3$$

Springs

Let $\mathbf{d}_{n,m}=\mathbf{X}_n-\mathbf{X}_m$ be the vector pointing from particle n to particle m and let $d_{n,m}=|\mathbf{d}_{n,m}|$ be the distance from particle n to particle m. For those particles n and m connected by an elastic link we define the rest length $r_{n,m}(t)$ to be the distance at which the link between them is relaxed. At t=0, we assume that all springs are relaxed, i.e., $r_{n,m}(0)=d_{n,m}(0)$. Let d be the characteristic length scale of the springs at rest defined by the mean distance between connected particles at time t=0. Let I be a matrix with entries $I_{n,m}$ for row n and column m with a value equal to either 0 or 1 in the case that

particle n and m are connected or not, respectively. To calculate the total force at particle n we write its local force density by:

$$\mathbf{f}_n = \frac{1}{\mathrm{d}_0}\sum_{m=1}^{N_p} I_{n,m}\frac{\mathbf{d}_{n,m}}{d_{n,m}}T_{n,m} \tag{7}$$

where $T_{n,m}$ is the force of a spring per area element of a node. We assume the area element of a node to be $\sim d_0^2$ (recall that the surface area of a sphere with radius d_0 is $\sim d_0^2$), thus the discrete surface tension of a spring per nodal area is set to be:

$$T_{n,m} = \frac{k_{n,m}}{\mathrm{d}_0^2}(d_{n,m} - r_{n,m})$$

where $k_{n,m}=k_{n,m}(t)$ is a hookean coefficient for a spring connecting particles n and m. The spring model used in this paper is simplified to illustrate basic concepts of the immersed boundary method in biofilm modeling. The general framework of IB easily allows for extension to include more sophisticated spring types, e.g., nonlinear viscoelastic). We set parameters as follows: imagine a block of biomass, which is attached to the substratum and then subjected to a shear force F. The block of biomass is distorted such that its top surface moves a distance ΔW. If H is the height of the biomass and A is the area of the top surface, then the shear modulus is defined as $G = \frac{F/A}{\Delta W/H}$. The spring coefficient has been chosen such that the shear modulus is approximately of the order of 1Pa, consistent with rheological measurements. In future studies we plan an extended model with springs according to Jeffrey's law that will include spring dampening and long time relaxation. To match properties to measurements of biofilm behavior we intend to calibrate with data from Shaw *et al.* (2004). For an evaluation of viscoelastic network behavior with respect to different spring models see Bottino (1998). The behavior of our computational biofilm should be independent of a refinement of the continuum representation in Figure 1 with respect to discretization refinement, i.e., number of springs per area (2D) or per volume (3D). This is achieved by scaling the spring coefficient with the nodal mean distance such that $k\sim d_0$ in 2D and $k\sim d_0^2$ in 3D. For the computational sloughing experiment a simplified approach was adopted for describing detachment of biomass. When a spring between two connected particles extends beyond a given length, i.e., reaches a critical strain, then the spring is assumed to break. For definiteness we defined the breaking length to be twice the resting length, i.e., springs for which $d_{n,m}(t) > 2r_{n,m}(t)$ are removed from the system.

Table 1. Model parameters and constants.

Parameter	Symbol	Value	Physcial unit
Height	H	$300\cdot10^{-6}$	m
Kinematic viscosity	ν	$1.004\cdot10^{-6}$	m^2/s
Density	ρ	998.3	kg/m^3
Top plate velocity	U	10^{-3}	m/s
Spring coefficient	k	$66.750d_0$	kg/s^2

Numerical procedure

Given a fluid velocity **u**(t) and the position of particles **X**(t) the computational sub steps for each time step are:

1. Solve equation (6) for $\mathbf{X}_j(t+\Delta t)$ using first order Euler integration.
2. Calculate the N_p forces $\mathbf{f}_n(t)$ acting at the particles due to spring forces using equation (7).
3. Transmit internal nodal forces to the surrounding fluid by calculating the eulerian density-force field $\mathbf{F}_{i,j,k}$ at each (x_i,y_j,z_k) using equation (4).
4. Solve the Navier-Stokes equations (1) and (2) to obtain $\mathbf{u}(t+\Delta t)$.

Our numerical framework for step (4) has been developed using the projection method (Chorin (1968)) for the Navier-Stokes equation. The code does not include any commercial components and

has been developed solely by the authors. Time discretization follows the first order Euler method. To improve stability restrictions on the time step Δt, the viscous term $\nu\nabla^2\mathbf{u}$ is handled implicitly using the ADI method Peaceman and Rachford (1955).

RESULTS AND DISCUSSION

Conceptual example

At time t=0 the continuum structures of Figure 2(a), consisting of an attached biofilm colony and a flock, are discretized using 920 particles distributed over the two shapes. Particles are perturbed as in Figure 1 and interconnected by 4651 springs, Figure 2(b). At y=0 springs are also added connecting the biofilm to the substratum. The upper channel boundary y=300μm is set in motion with speed 10^{-3} m/s. System flow is computed in the computational domain. Momentum transfers from the top boundary into the bulk fluid-biofilm system. At t=0.0672s, Figure 2(c), the bulk fluid has started to move near the biofilm. By t=2.87s, Figure 2(d), shear stress from the top boundary has transmitted to the bulk fluid and then to the biofilm, resulting in strain. Note the small free floating flock that advects freely through the bulk fluid-there are no forces other than those from the surrounding bulk fluid that affect its path, allowing it to flow past the rectangular shaped biofilm at t=8.87s, Figure 2(e). At t=11.6s, Figure 2(f), the rectangular biofilm is close to a steady state. At this point in time, forces from the substratum are balanced by forces from the fluid flow, i.e., the flow field inside the rectangular colony has almost reached zero. The free floating colony has passed by the attached colony traveled an entire domain length and crossed the periodic boundary.

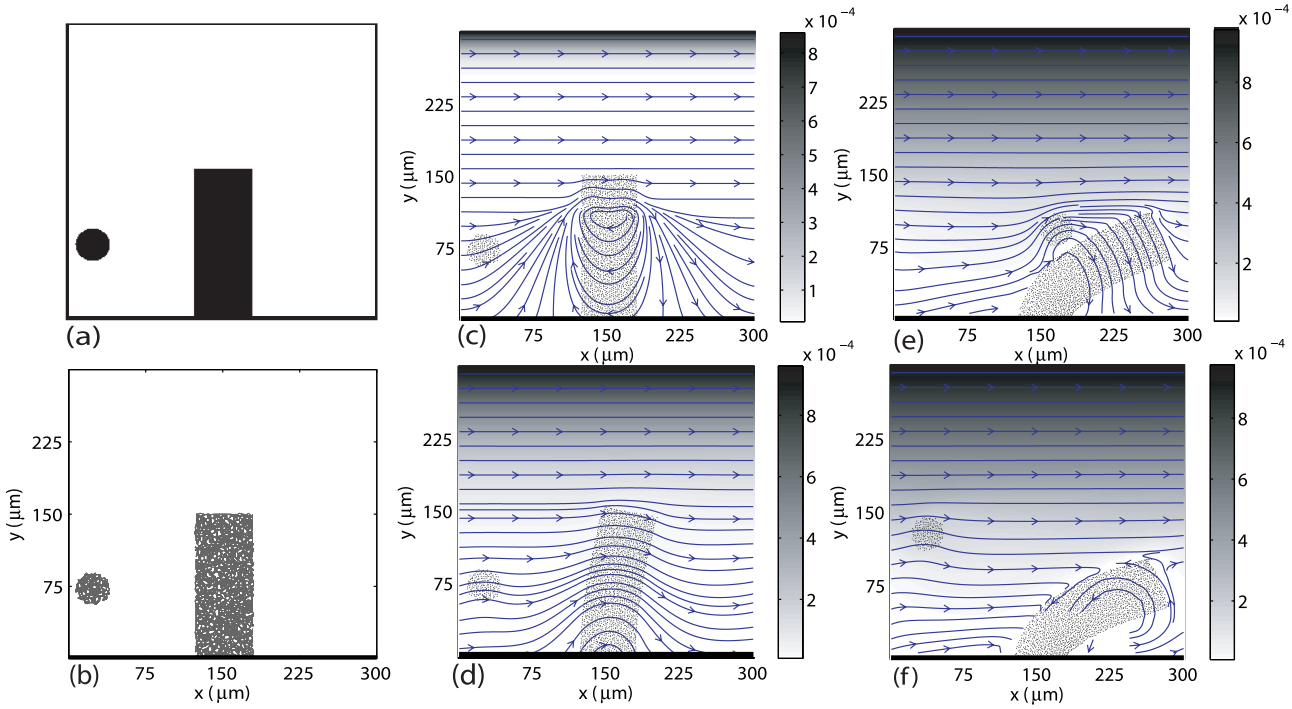

Figure 2. An example of an artificially shaped 2D biofilm in the form of a rectangular block and a free floating circular flock evolved in time using the IB method. Left (a) shows the initial continuum shape and (b) its discretized version. In (c), (d), (e) and (f) flow speed and instantaneous streamlines can be seen at time t=0.0672s for (c), t=2.87s for (d), t=8.87s for (e) and t=11.6 for (f).

2D streamer

A biofilm shaped to perform and interact with the bulk fluid flow as a streamer was constructed, see Figure 3(a). The initial structure was composed of a towering colony, which we refer to as a streamer, along with two smaller nearby colonies. For this particular simulation the speed at

y=300μm was set to 10^{-3} m/s from time t=0s to t=3s at which time the speed there is reset to zero. At t=0.28s, Figure 3(b), the bulk flow can be seen to interact with the biofilm as its structures block the flow, creating a whirlwind-like movement within the flow of the towering-structure. At t=1.48s, Figure 3(c), the streamer starts to bend, transferring fluid momentum into stored elastic energy. At t=2.98s, Figure 3(d), the streamer has been stretched across the computational domain. After flow at has stopped, the streamer pushes backwards toward its initial position. At t=15s, Figure 3(e),

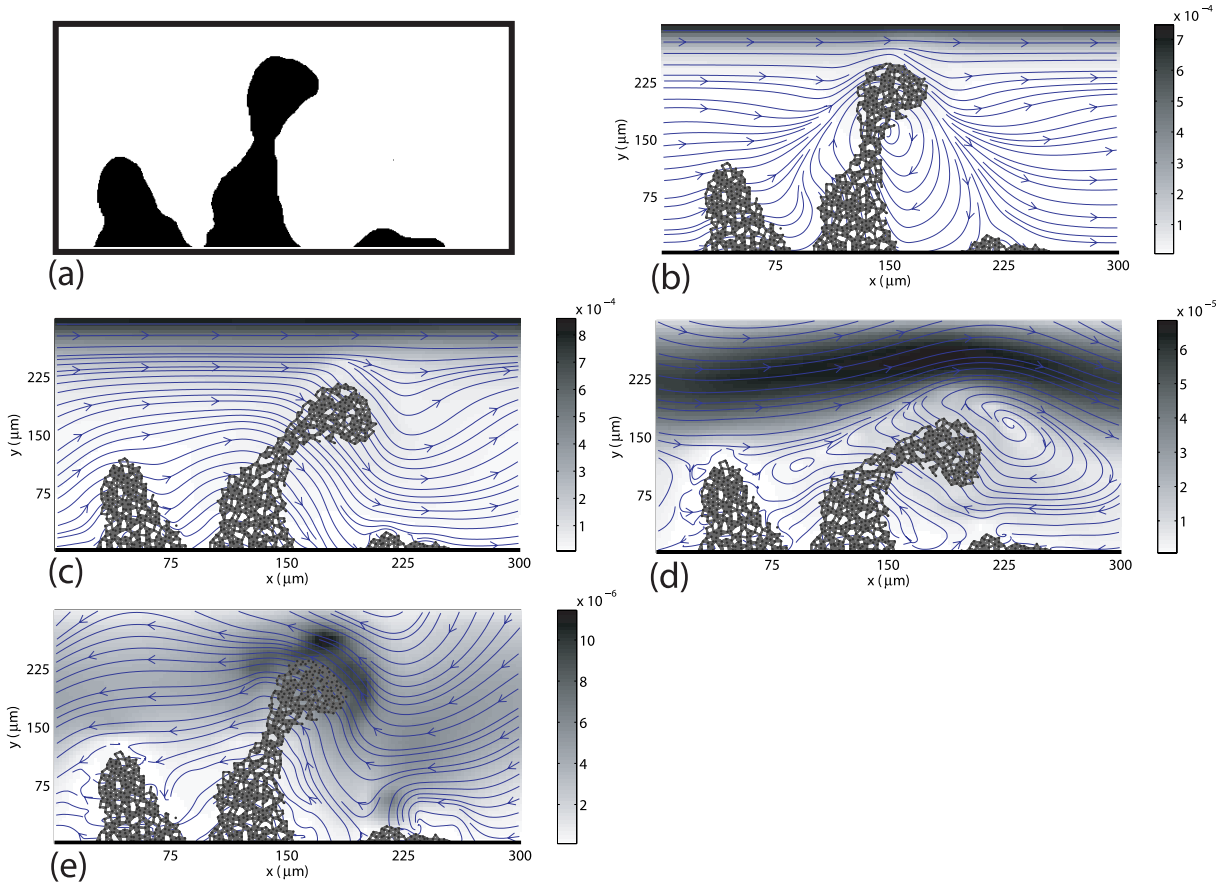

Figure 3. Simulation of a 2D streamer with (a) the initial undiscretized structure. Plots (b)-(e) show instantaneous streamlines of the liquid flow and the norm of velocity speed in m/s at times t=0.28s, t=1.48s, t=2.98s and t=15s.

3D sloughing biofilm

A fictional "mushroom" shaped biofilm was constructed using silhouette carving from two binary images. The continuum shapes were discretized with 7146 particles connected by 67816 springs; see Figure 4(a). At t=0s the biofilm was subjected to flow of 10^{-3} m/s and interaction of flow and biomass begins. Observe how at t=3.27s, Figure 4(b), biomass starts deforming in the direction of the flow field. From Figure 4(e) it is clear that the top of the mushrooms acts as an obstacle to flow even though at this point in time, the mushroom is still not in steady-state. At t=4.07s, Figure 4(c), mushroom is compressed along the x-dimension. In Figure 4(f) the force density exerted by the biofilm is shown. Note that it is highest at the top (where strong bulk fluid shear is present) and also at the biofilm-substratum interface (where elastic stress is transferred). Force density is high close to the small cavity near the bottom of the biofilm. At this particular location, the number of springs per volume is small compared to that of other places within the biofilm, hence large individual forces occur in the springs, resulting in susceptibility to rupture and detachment. In Figure 4(d), at time t=5.67s, the mushroom shaped structure has completely detached from the substratum. The detached part now is tumbling down on top of the smaller colony exerting force and momentum transfer on it. The impact and subsequent momentum transfer causes the smaller colony to detach.

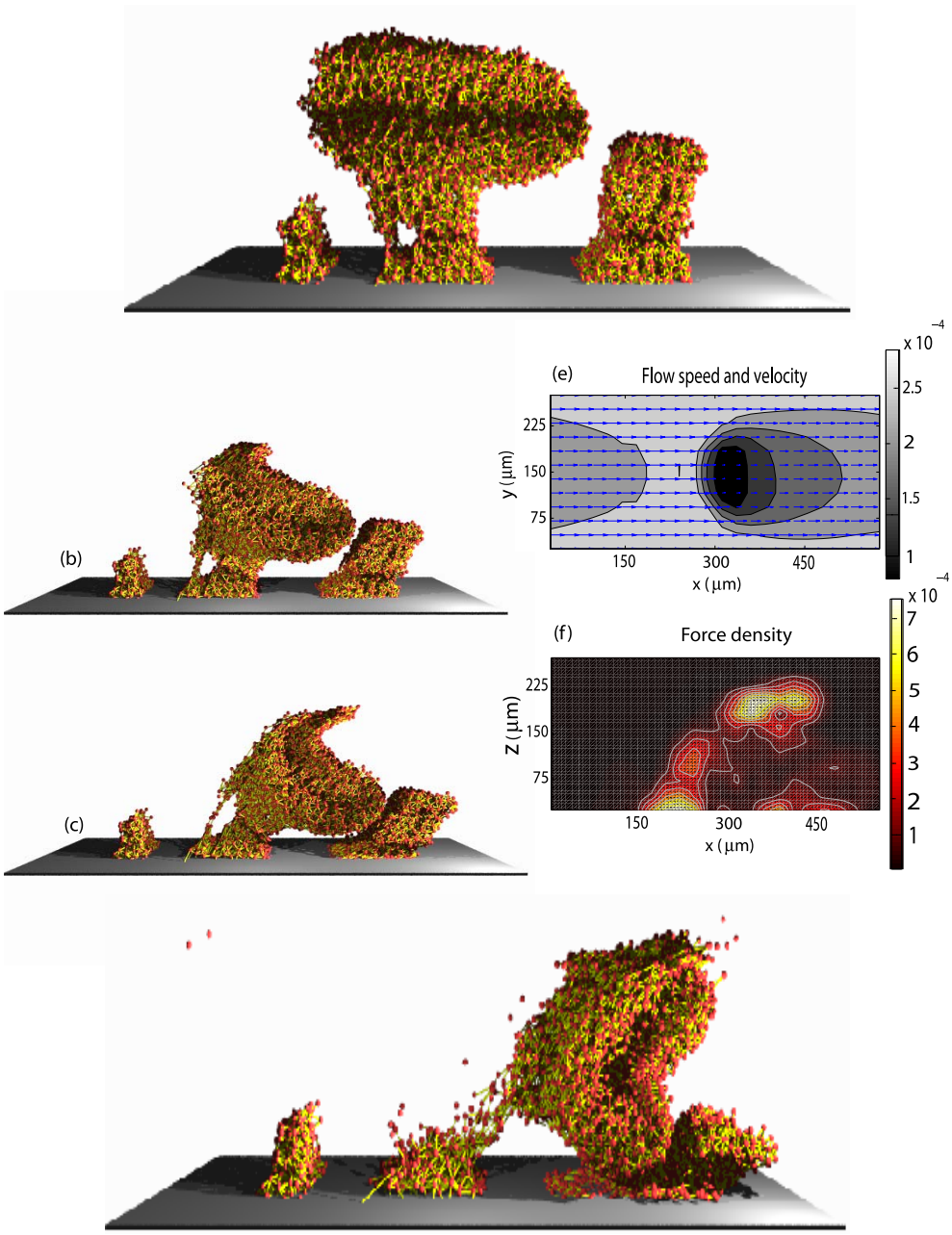

Figure 4. A fictionally shaped biofilm detaching under impact of flow (a)-(d). (e) show the flow and velocity of biomass and liquid in the plane at z=286µm, t=3.27s. In (f) the force density is illustrated at y=143µm in N/m^2, t=4.07s. (b)-(d) are snapshots at times t=3.27s, t=4.07s, and t=5.67s respectively.

CONCLUSIONS

In this paper we have presented a new and novel approach to modeling interaction between fluid flow and biomass. This is the first step towards a macro scale particle biofilm model which includes the mechanical coupling with bulk fluid shear flow. Such interaction, particularly through shear stress modulated momentum transfer, is essential for a correct description of biofilm sloughing and hence for a correct description of the long-time behavior of biofilm-bulk fluid systems. To accomplish this we utilize the immersed boundary method for describing the biomass and fluid flow interaction. With the method of immersed boundary, it is possible to simulate liquid flow and biomass interaction in 3D. At the current stage the model is capable of describing free floating biofilm objects, streamers and detachment processes, while obeying fundamental principles of physics, namely conservation of mass and momentum.

ACKNOWLEDGEMENTS

I.K. was supported by NIH award 5R01GM67245 and E.A. acknowledges the financial support of the KK foundation. The authors would like to thank IPAM for its hospitality.

REFERENCES

Alpkvist E. and Klapper I. (2006). A multidimensional multispecies continuum model for heterogeneous biofilm development. *Submitted to Bull. of Math. Biol.*

Alpkvist E., Piciroreanu C., Loosrecht MCM. and Heyden A. (2006). Three-dimensional biofilm model with individual cells and continuum eps matrix. *In press Biotech. Bioeng.* (2006).

Batchelor G. *An Introduction to Fluid Dynamics*. (1967). Cambridge University Press.

Bottino D. (1998). Modeling viscoelastic networks and cell deformation in the context of the immersed boundary method. *J. Comput.Phys.* **147**(1), 86 -113.

Chambless J., Hunt S. and Stewart P. (2006). A three-dimensional computer model of four hypothetical mechanisms protecting biofilms from antimicrobials. *Appl. Environ. Microbiol.* **72**(3)**,** 2005–2013.

Chorin A. (1968). A numerical solution of the navier-stokes equations. *Math. Comp.* **22**, 745–762.

Cogan N. (2006). Hybrid numerical treatment of two fluid problems with passive interfaces. *Preprint*.

Dillon R., Fauci, L. and Gaver D. (1996). Modeling biofilm processes using the immersed boundary method. *J. Comput. Phys.***129**(1), 57–73.

Dockery J. and Klapper I. (2001). Finger formation in biofilm layers. *SIAM J. Appl. Math.* **62(**3), 853–869.

Eberl H., Parker D. and Van Loosdrect MCM. (2001). A new deterministic spatio-temporal continuum model for biofilm development. *J. Theor. Med.* **3**, 161–175.

Fogelsson A. L. and Guy R. D. (2004). Platelet wall interactions in continuum models of platelet thrombosis: formulation and numerical solution. *Mathematical Medicine and Biology* **21**(4), 293-334.

Gurtin M. (1981). *An Introduction to Continuum Mechanics*. Academic Press.

Klapper I. Rupp C., Cargo R., Purvedorj B. and Stoodley P. (2001). Viscoelastic fluid description of bacterial biofilm material properties. *Biotech. Bioeng.* **80**(3), 289–296.

Peaceman D.W. and Rachford J. H. H. (1955). The numerical solution of parabolic and elliptic differential equations. *J. Soc.Indust. Appl. Math.* **3**, 28–41.

Peskin C. (1977). Numerical analysis of blood flow in the heart. *J. Comp. Phys. 81*, 372–405.

Peskin C. (2002). The immersed boundary method. *Acta Numerica*, 479–517.

Picioreanu C., Van Loosdrecht MCM. and Heijnen J. (1998). Two-dimensional model of biofilm detachment caused by internal stress from liquid flow. *Biotechnol. Bioeng.* **72**, 205–218.

Picioreanu C., Van Loosdrecht MCM. and Heijnen J. (1998). Mathematical modeling of biofilm structure with a hybrid differential-discrete cellular automaton approach. *Biotechnol. Bioeng.* **58**, 101–116.

Shaw T., Winston M., Rupp C. Klapper I. and Stoodley P. (2004) Commonality of elastic relaxation times in biofilms. *Phys. Rev. Lett.* **93(**9), 1–4.

Stoodley P., Cargo R., Rupp C. and Klapper, I. (2002). Biofilm material properties as related to shear-induced deformation and detachment phenomena. (2002). *J. Ind. Microbiol. Biotechnol.* **29**(6), 361–367.

Wloka M., Rehage H., Flemming H. and Wingender J. (2004). Rheological properties of viscoelastic biofilm extracellular polymeric substances and comparison to the behavior of calcium alginate gels. *Colloid and polumer science* **282(**10), 1067–1076.